THE IFR DETECTOR AT SuperB*

Jaroslaw Wiechczynski

The Henryk Niewodniczański Institute of Nuclear Physics
Polish Academy of Sciences
Radzikowskiego 152, 31-342 Kraków, Poland

(Received May 10, 2012)

The SuperB project is an international enterprise aiming at the construction of the high-luminosity asymmetric beam energy electron–positron accelerator, along with the dedicated detection system. The Instrumented Flux Return (IFR) is the subdetector designed primarily for the purposes of the muon identification. In this paper, the main physical goals are discussed and the overview of the baseline design for the IFR detector is given. Also, the IFR prototype and the studies on the test-beam data are presented.

DOI:10.5506/APhysPolB.43.1653
PACS numbers: 07.77.Gx, 13.20.He, 14.60.Ef, 29.40.Mc

1. Introduction

The SuperB detector [1] consists of various subdetectors devoted for specific physical goals. They are Silicon Vertex Tracker (SVT), Drift CHamber (DCH), Particle IDentification (PID), ElectroMagnetic Calorimeter (EMC) and — the outermost part of the SuperB detection system — Instrumented Flux Return (IFR) (Fig. 1).

The main goal of the IFR system is to identify muons and, along with the electromagnetic calorimeter, to detect neutral hadrons such as K_L^0 mesons. The iron yoke of the detector magnet consists of the large amount of material to absorb hadrons and provides a segmentation in depth. The gaps between each segment are to be filled with detection layers for the measurement of the penetration depth.

2. Physical purposes

The SuperB experiment aims for the several interesting measurements, which would be crucial for the search of the New Physics beyond the Standard Model and which depend on the efficient performance of the IFR

* Presented at the Cracow Epiphany Conference on Present and Future of B Physics, Cracow, Poland, January 9–11, 2012.

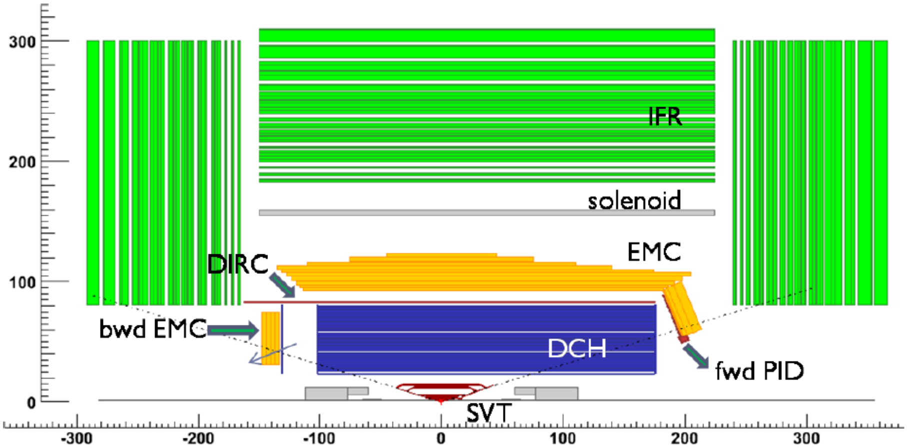

Fig. 1. The SuperB detector with the outermost IFR apparatus (dark grey/green).

apparatus. Namely, the transitions $b \to sl^+l^-$ and $b \to dl^+l^-$ require the good discrimination between penetrating particles (muons) and the charged hadrons like pions and kaons, that can form significant background contribution to the signal events. High efficiency of the muons identification is also crucial to search for lepton flavour-violating processes (*e.g.* $\tau \to \mu\gamma$) as well as in the studies of rare B decays such as $B \to \tau\nu_\tau(\gamma)$, $B \to \mu\nu_\mu(\gamma)$ and $B_d(B_s) \to \mu^+\mu^-$. Concerning the above final states with missing energy (carried by neutrinos), the critical issue is the suppression of the background coming from the decays, in which the energy is carried by the neutral hadrons. Hence, the good identification of such hadrons (like K_L^0) plays an important role in the construction of the IFR detector.

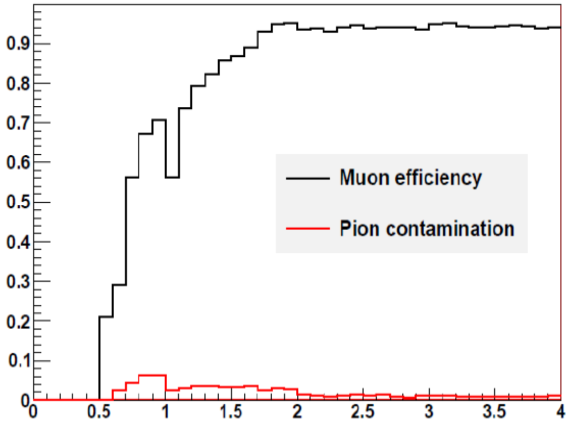

Fig. 2. Efficiency of the muon identification and the fraction of pion contamination based on the Monte Carlo studies.

Fig. 2 shows the efficiency and probability of the misidentification for muons and charged pions, in the function of the particle's momentum. This preliminary result is based on the Geant4 [2] simulations with the cut based muon selector. One can conclude that for the momentum higher than 2 GeV the efficiency for muon identification exceeds 95%, while the fraction of the pion contamination is less than 5%.

3. Detector overview

The IFR detector is built in the magnet flux return and consists of one hexagonal barrel-like structure and two endcaps. In the SuperB baseline configuration the thickness of the absorbing material is 920 mm, which corresponds to the 5.5 interaction lengths. Such material is interleaved by 8(9) active layers of highly segmented scintillators. The signal from the extruded scintillator bars is a readout through three wavelength shifting (WLS) fibers and Silicon Photo-Multipliers (SiPM). In order to achieve the best possible efficiency of the light detection and simplicity of the detector design, various SiPM types are under investigation. In addition, the newer technology of the Multi Pixel Photon Counters (MPPC) is studied for the utility of the IFR readout system [3].

The baseline design foresees the reuse of the flux return system coming from the BaBar experiment, however, the existing apparatus is not optimal for muon identification [4] so several modifications need to be made in order to achieve the desired thickness of the detector. This could be made either by filling existing gaps with additional iron plates (brass or steel) or by adding material to the external surface of the detector.

3.1. The IFR readout system

The baseline option for the IFR assumed to use two different readout types: a Time Readout (TDC-RO) and a Binary Readout (Bi-RO). In the Time Readout, proposed for the barrel-like part of the detector, each active layer consists of 4 meters long and 2 cm thick scintillator bars that could be read at both ends. The azimuthal coordinate ϕ would be measured from the hit bar, while the polar angle Θ would be determined from the arrival time of the signal digitized by the Time to Digital Converter (TDC). However, this option implicates the limited resolution for the polar coordinate due to time resolution of the TDC system (~ 1 ns), which gives the spatial uncertainty of the order of 20 cm.

In the Binary Readout, assumed for the endcaps, the particle track is to be measured by two orthogonal 1 cm thick layers, where each scintillator bar is 2 meter long and can be read out only at one end. After the studies on the prototype results (see next section) the IFR group proposed the new readout option, dropping the TDC-RO and use the Binary Readout for both barrel and endcaps structures of the detector. Fig. 3 illustrates the difference between those two approaches for the barrel's readout method.

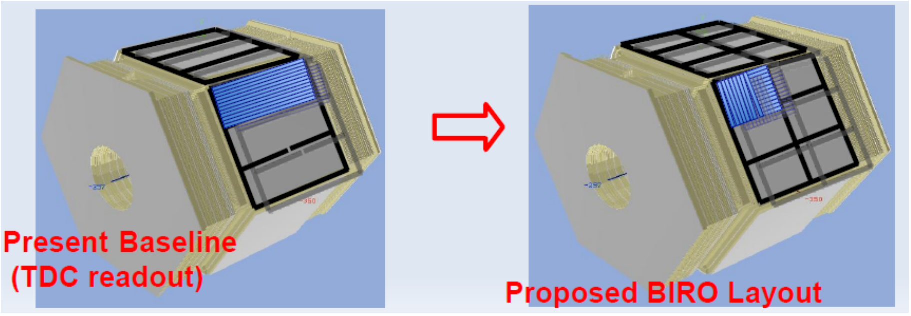

Fig. 3. The illustration of the baseline readout system for the barrel structure (Time Readout — left plot) and the new proposed option (Binary Readout — right plot).

4. The IFR prototype

The prototype is a structure composed by the full stack of iron, segmented with 3 cm gaps to house the active layers. The size of the prototype is $60{\times}60{\times}92$ cm^3 and it contains 9 active layers: 5 Binary Readouts and 4 Time Readouts. Fig. 4 shows the prototype scheme and three coordinates introduced (X, Y, Z).

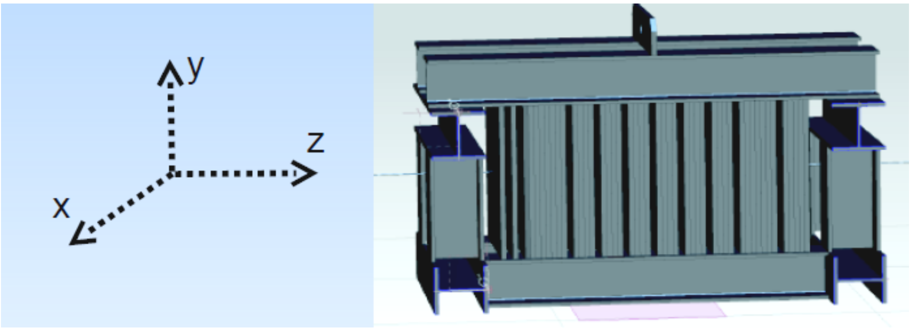

Fig. 4. The IFR prototype scheme along with its coordinates system.

The main purposes of the construction of the prototype include studies of different detector configurations, validation of the simulation results by performing muon/pion separation on real data and the studies on the hadronic shower development. Such results are important for the detector geometry optimization (its segmentation, amount of material, *etc.*) and, on the other hand, gives a valuable input for the full simulations.

So far, several beam-tests have been done at Fermilab laboratory using a muon/pion beam of the different momentum. The scheme of the test-beam setup is presented in Fig. 5.

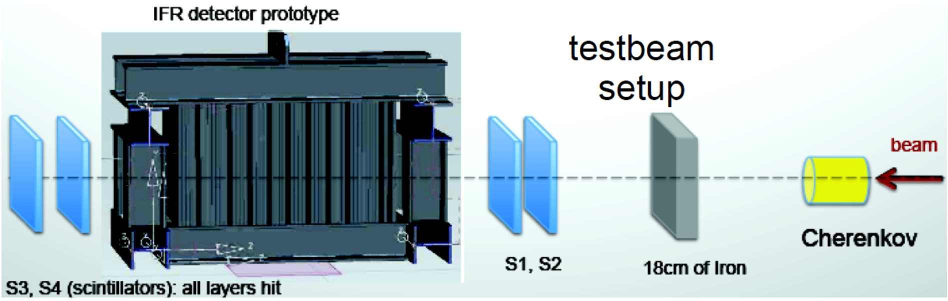

Fig. 5. Test-beam setup for the IFR prototype. The elements from the right to left are as follows: Cherenkov detector used for muon/pion separation and for electron veto; iron block for the electron absorption; S1 and S2 scintillators that serve as trigger detectors and provide the reference time; the prototype; S3, S4 scintillators indicate that the particle activated all the layers of the prototype.

4.1. The prototype data analysis

The participation in the analysis of the prototype data is one of the tasks performed by the author of this paper. This mainly includes the selection of the muon-like events, separation between the muon pattern and the background (noise) hits, followed by the fitting procedure to determine the muon track. Fig. 6 shows the prototype response to the muon and pion events, which differ by the number of hits in the active layers and the depth of the penetration in the prototype. Further steps in the data analysis are checking the residual distribution for the detector's alignment studies and preliminary efficiency calculations on the layer level.

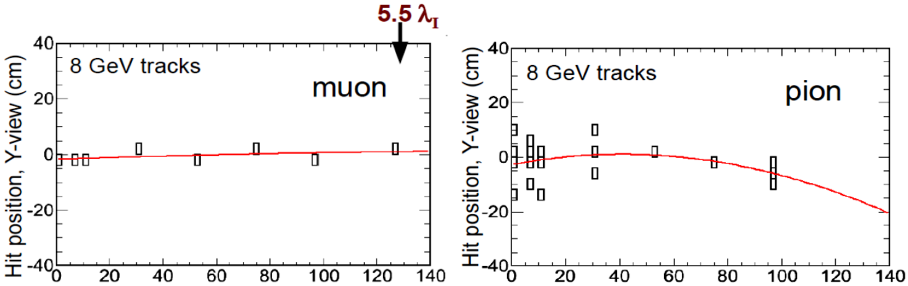

Fig. 6. Example of muon-like (left plot) and pion-like (right plot) events from the prototype data.

4.2. Clustering algorithm

In order to remove the background hits and identify the good muon track, the clustering algorithm based on the K-means method [5] is used. For the purpose of this analysis, two planes (views) of the prototype (XZ and YZ) are considered separately. For the YZ view, each layer has a Binary Readout, whereas for XZ plane both Binary and Time Readouts are included, for even and odd layers, respectively[1]. The details of the clustering algorithm are given below.

In order to clusterize the YZ plane, the initial so-called centroids are introduced every 5 cm, so that each hit in the event can be assigned to the closest centroid. In the next step, the positions of the centroids are recalculated as the weighted average of the assigned hits and the assignment is repeated. The procedure continues until no single hit changes its centroid, so the final clusters are formed. Then the cluster with the highest occupation is chosen and it is merged with the adjacent ones if their positions are within the given distance from the most crowded cluster. Such newly created big cluster is considered to contain hits coming from the propagating muon. All remaining distant clusters correspond to the background hits. Fig. 7 demonstrates two main steps of the clusterizing method described above.

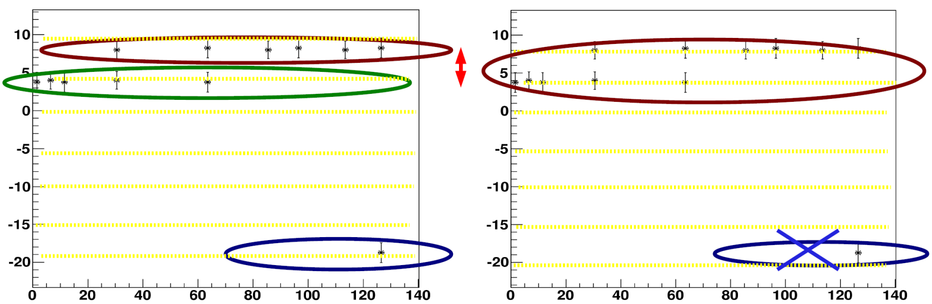

Fig. 7. The illustration of the clustering procedure based on the K-means algorithm. Left plot shows three clusters introduced by the positions of the hits. Right plot presents the merged cluster (recognized as the good muon pattern) and the less populated cluster interpreted as containing the background hit.

The XZ plane, containing both Bi-RO and TDC-RO hits, is clusterized in two steps. Firstly, only the Binary hits are chosen and the noise hits are identified among them, in exactly the same way as for the YZ view. Once it is done, the TDC-RO hits (of 20 cm uncertainty) are added to the good Bi-RO track and a new coarser centroids (placed every 20 cm) are introduced. Afterwards, the new clusters containing hits of both readout

[1] The layers are counted from 0 to 8.

types are formed and the one including the proper Bi-RO track is considered as the pattern of muon. Likewise, the adjacent TDC-RO clusters may be added to this pattern if their distance from the main cluster is less than certain value.

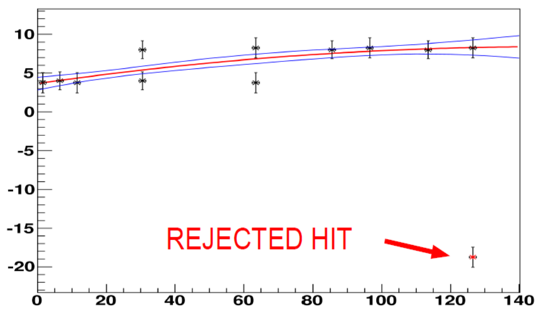

Fig. 8. Fit to the hits forming good muon track, as recognized by the clustering algorithm. The second order polynomial is used as the fitted function. The middle/red curve and the outer/blue curves indicate the fitted track and its uncertainty region, respectively.

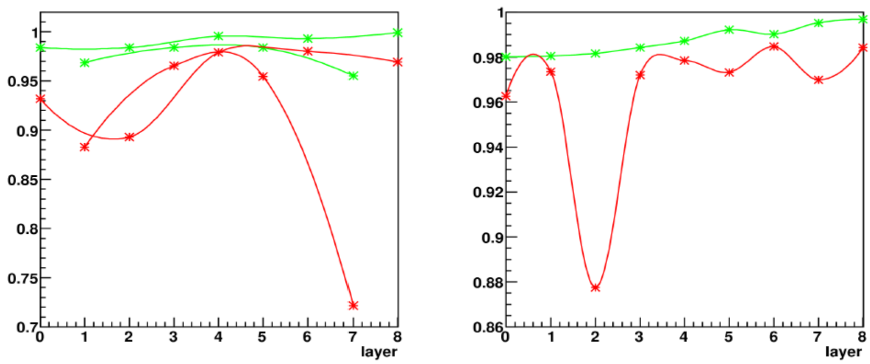

Fig. 9. Plot of the efficiency for each layer, for XZ (left) and YZ (right) view, calculated for the prototype data with the 8 GeV muon beam. Light grey (green) curves represent the fraction of hits which lie within 3 sigma of the fitted track (1.5 sigma for the TDC-RO hits) and can be considered as the test of the clustering method's performance. Grey (red) curves indicate the absence of the hit within 3(1.5) sigma of the fitted track, for each layer. 1 sigma is defined as quadratic sum of the hit uncertainty and the error of fitted track at given layer.

The clustering algorithm was firstly prepared as the independent procedure, and then it was implemented into the IFR software for the analysis of the prototype data from the last test-beam.

After the signification of the muon is found for XZ and YZ planes, the second order polynomial function is fitted to the relevant hits for both views. Fig. 8 presents an example of the fit performed to the hits selected for the YZ plane.

From the fits performed to the significant sample of clusterized muon-like events, one can obtain the efficiency (Fig. 9) and the residual distributions (Fig. 10) for each layer, for both XZ and YZ planes.

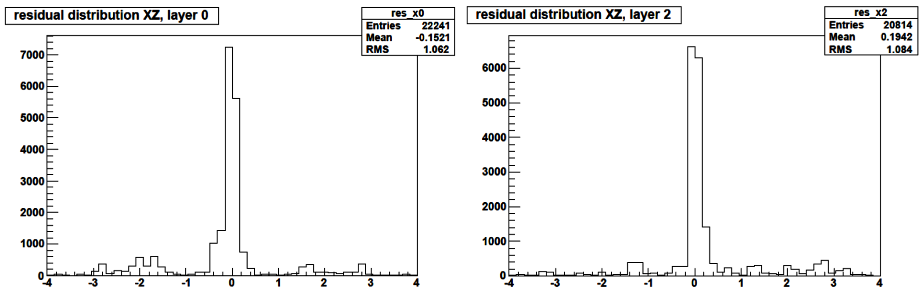

Fig. 10. Example of the residual distribution for the XZ plane, for layer 0 (left plot) and layer 2 (right plot). To obtain such plots, the distance between each hit (accepted by the clusterizer) and the fitted track is histogrammed.

5. Summary

The studies on the design and optimization of the IFR detector are now in an advanced progress. Based on the information collected from these studies and from the analysis of the data from the last test-beam (performed in Ferbruary 2012) the Technical Design Report (TDR) is expected to be prepared this year.

I would like to thank Tadeusz Lesiak for his support. I would also like to express my gratitude to the IFR group from Ferrara, especially to Gianluigi Cibinetto for the fruitful discussions.

REFERENCES

[1] E. Grauges, F. Forti, B. Ratcliff, D. Aston [SuperB Collaboration], `arXiv:1007.4241v1 [physics.ins-det]`.
[2] S. Giani *et al.*, GEANT4: An Object-Oriented Toolkit for Simulation in HEP, CERN/LHCC/98-44.
[3] C. Piemonte *et al.*, *Nuovo Cim.* **C30**, 473 (2007); MPPC specs at: `http://sales.hamamatsu.com/en/products/solid-state-division/si-photodiode-series/mppc.php`
[4] B. Aubert *et al.*, *Nucl. Instrum. Methods Phys. Res.* **A479**, 1 (2002).
[5] Cluster Analysis: Basic Concepts and Algorithms, `http://www.aw-bc.com/info/kumar/assets/downloads/ch8.pdf`